Influence of Levofloxacin and Clarithromycin on the Structure of DPPC Monolayers

Stephanie Ortiz-Collazos,[1] Paulo H. S. Picciani,[2] Osvaldo N. Oliveira Jr,[3] Andre S. Pimentel,[1*] and Karen J. Edler [4]

1. Departamento de Química, Pontifícia Universidade Católica do Rio de Janeiro, Rio de Janeiro, RJ 22453-900 Brazil
2. Instituto de Macromoléculas Professora Eloisa Mano, Universidade Federal do Rio de Janeiro, Rio de Janeiro, RJ 21941-598, Brazil
3. Instituto de Física de São Carlos, Universidade de São Paulo, CP 369, 13560-970 São Carlos, SP, Brazil
4. Department of Chemistry, University of Bath, Claverton Down, Bath BA2 7AY, UK

*Corresponding author: a_pimentel@puc-rio.br

Abstract

Research on lipid/drug interactions at the nanoscale underpins the emergence of synergistic mechanisms for topical drug administration. The structural understanding of bio-mimetic systems employing 1,2-dipalmitoyl-sn-glycero-3-phosphocholine (DPPC) as a lung surfactant model mixed with antibiotics, as well as their biophysical properties, is of critical importance to modulate the effectiveness of therapeutic agents released directly to the airways. In this paper, we investigate the structural details of the interaction between Levofloxacin, 'a respiratory quinolone', and the macrolide Clarithromycin, with DPPC monolayers at the air-water interface, using a combination of Brewster angle microscopy, polarization modulation-infrared reflection-adsorption spectroscopy (PM-IRRAS), surface pressure isotherms and neutron reflectometry (NR) to describe the structural details of this interaction. The results allowed association of changes in the π-A isotherm profile with changes in the molecular organization and the co-localization of the antibiotics within the lipid monolayer by NR measurements. Overall, both antibiotics are able to increase the thickness of the acyl tails in DPPC monolayers with a corresponding reduction in tail tilt as well as to interact with the phospholipid headgroups as shown by PM-IRRAS experiments. The effects on the DPPC monolayers are correlated with the physical-chemical properties of each antibiotic and dependent on its concentration.

Keywords: lung surfactant model, monolayer, macrolide, fluoroquinolone, phospholipids, neutron reflectometry.

Introduction

Interest in investigating the interactions between biological interfaces and bioactive compounds is increasing, mainly due to their importance in nanotechnology and medicine. Lung surfactant (LS) is a complex lipoproteic fluid secreted by pneumocytes cells type II lining the alveolar air-water interface of the lung(1). The LS function is to lower the surface tension to values close to 0 mNm^{-1} and thus prevent alveolar collapse. To achieve low surface tensions the LS forms a monolayer enriched mostly in 1,2-dipalmitoyl-sn-glycero-3-phosphocholine (DPPC), responsible for the stability, high packing density and surface active function of the film at the end of expiration(2). The lack or dysfunction of LS is frequently associated with the presence of pathogens that can interact directly with the surfactant film and impair its properties. Acute respiratory distress syndrome (ARDS) is a severe condition of pulmonary insufficiency due to a deficiency of alveolar surfactant along with structural immaturity of the lungs(3). Thus, ARDS affects mainly, but not exclusively, preterm babies. Adult patients with pneumonia, sepsis and serious lung trauma can also develop it(4). Exogenous lung surfactant is an organic extract of porcine/bovine lungs used as a replacement therapy for the natural one for the treatment of ARDS and many other clinical conditions. However, there is also a risk that exogenous lung surfactant will be inactivated in the presence of infectious agents. Due to this, the use of exogenous surfactant mixed with antibiotics has been suggested as a platform for delivering therapeutic agents directly to airways based on its rapid spreading properties(5). However, there is little information related to the structural parameters of LS monolayers at the nanoscale, which can be affected by the presence of therapeutic agents and so should be investigated in more detail.

The Langmuir technique allows formation of phospholipid monolayers at the air-water interface which may be used as the simplest model of a lung surfactant to investigate the interactions with species such as drugs, toxins or pollutants(6–9). This approach is especially convenient since the monolayer stability may be investigated(8–11) and the compounds can be purposefully added to the subphase at a controlled concentration(8, 12, 13) or mixed with the lipid monolayer(9). 1,2-dipalmitoyl-sn-glycero-3-phosphocholine (DPPC) is one of the most important and abundant phospholipid occurring in lung surfactant. Its monolayer at the air-water interface is well characterized(14, 15). Therefore, this phospholipid is often used as a model of the outer

cell membrane leaflet, (7, 16, 17) lung surfactant bilayers(18) and monolayers(19, 20) to get insights about membrane properties and the interactions between its components.

The significance of investigating the interactions between lung surfactant models with antibiotic agents relies on the understanding of how its biophysical interplay affects the lipid membrane structure, its organization, and mechanical properties, which, ultimately, will have an effect on the functionality of the mixed system on disrupting the lung surfactant. In this sense, Neutron reflectometry (NR) is a powerful technique to examine the structure of amphiphiles normal to the interface and provides valuable contrast variation measurements for the structural description and characterization of mixed systems such as lipid membrane models(21, 22). Indeed, DPPC is a phospholipid widely used to mimic the interfacial properties of lung surfactant at the air-water interface because it is the main LS constituent(23–27), thus it can reveal key information related to interactions with target molecules. For example, Fullagar *et al* applied NR on surfactant protein B (SP-B)/DPPC mixed films at the air-water interface to identify SP-B localization in the film as a function of surface pressure, as well as the squeeze-out process of the protein from the lipid monolayer(25). In the same line of reasoning, Follows *et al*, studied the organization and dynamics of LS preparations of bovine and porcine origin at the air-water interface by NR. These results showed that a multilayer structure can be formed in exogenous surfactant even at very low concentrations and suggested that multilayer models need to be incorporated into the current interpretations of *in vitro* studies.(26) On the other hand, some studies have used NR to examine the structure of asymmetric outer membrane models of Gram-negative bacteria *P. aeruginosa* as a mixed DPPC bilayer(28, 29); also its interaction with cyclic antibiotic lipopeptides has been further investigated by Han *et al*(30). However, as far as we know, the structural organization, stability and co-localization of antibiotics -such as fluoroquinolones and macrolides- on DPPC monolayers, as a simplified LS membrane model, have not been studied using the NR technique at the air-water interface.

In this work, the structural details of the interaction between Levofloxacin (a third-generation fluoroquinolone), as well as the semisynthetic macrolide Clarithromycin, with DPPC monolayers (acting as a membrane model) are studied at the air-water interface. Levofloxacin is catalogued as a “respiratory quinolone” due to the enhanced activity against the important respiratory pathogen *Streptococcus pneumonia*. Clarithromycin is a broad-spectrum antibiotic and one of the safest antibiotics available, mostly used to treat

infections of the upper and lower respiratory tract, including pneumonia and bronchitis(9). Some studies also suggest that aerosol formulation of Clarithromycin is an effective pulmonary drug delivery system for the treatment of respiratory infections(31). We have used NR, Brewster angle microscopy (BAM), polarization-modulation infrared reflection–absorption spectroscopy (PM-IRRAS) and Langmuir trough techniques to obtain new structural information about these mixed systems that can contribute to the design of new strategies in respiratory medicine.

Methodology

Langmuir monolayer studies

Fully hydrogenated and tail deuterated (d_{62}-) DPPC were purchased from Avanti Polar Lipids. Stock solutions of DPPC, with and without antibiotics, were prepared in HPLC grade chloroform (Sigma-Aldrich). The water used throughout the experiments was supplied by a Milli-Q Integral 10 purification system from Millipore (resistivity 18.2 MΩ.cm). Clarithromycin and Levofloxacin antibiotics (See structures in Figure 1) were donated by Aché Laboratórios Farmacêuticos. Monolayers of the neat lipid and mixed with the drugs were prepared by spreading 30 μL solution (1 $g.L^{-1}$ in chloroform) over a water subphase in a PTFE Langmuir trough (dimensions 300 x 75 mm^2) housed in a class 10,000 clean room. The Langmuir trough is coupled with two symmetrical mechanical barriers controlled by a Nima computer interface (KSV, Finland), and equipped with a Wilhelmy plate to measure surface pressure. A waiting time of 10 min was allowed for chloroform evaporation and monolayer equilibration, before the surface pressure - Area (π-A) isotherms were recorded at a compression rate of 10 mm min^{-1}. Mixed DPPC/antibiotic systems for each drug were prepared at three concentrations relative to DPPC stock solution (i.e., 0.1, 1 and 10%). The surface compressional modulus (Cs^{-1}), also known as the in-plane elasticity(32), was calculated from the surface pressure isotherms using the expression:

$$C_s{}^{-1} = -A\left[\frac{\partial \pi}{\partial A}\right]$$

where π is surface pressure and A is the mean molecular area. Isotherms were carried out both independent of, and in conjunction with, NR, BAM and PM-IRRAS measurements individually, at different surface pressures.

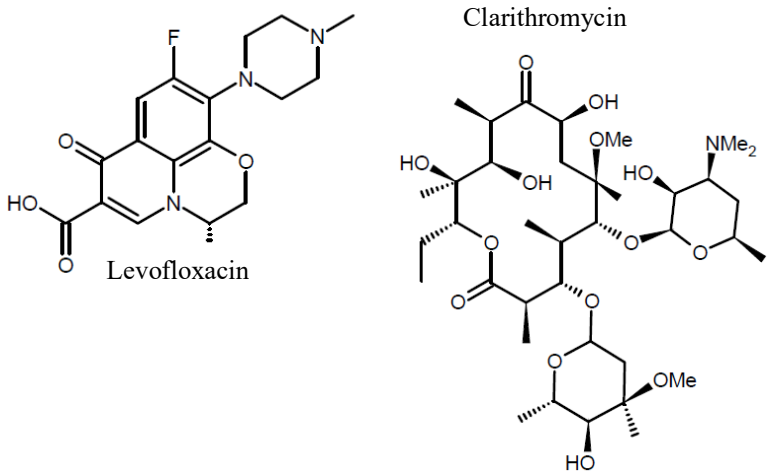

Figure 1. Molecular structures of the antibiotics used in this study.

Neutron reflectometry experiments

NR measurements were performed using the SURF reflectometer(33) on Target Station 1 at the ISIS Spallation Neutron Source at Rutherford Appleton Laboratory, Didcot, UK. Specular neutron reflectivity is largely determined by the variation in the scattering length density (SLD) along the surface normal. A reflectivity profile was recorded at two glancing angles of incidence, *viz.* 0.5° and 1.5°. Since neutron scattering is a nuclear effect, the scattering length varies for different isotopes, and therefore isotopic substitution can be used to obtain reflectivity profiles, corresponding to a single molecular density profile. This provides a means of determining the composition of multi-component systems, thus yielding detailed structural information of an adsorbed layer(34, 35). Pure DPPC and mixed DPPC/antibiotic monolayers were prepared and surface pressure measurements were used to monitor film compression. NR experiments were carried out at surface pressures of 5, 20, and 30 mNm^{-1} over an air-contrast matched water (ACMW) subphase (8% D_2O, 92% H_2O) on which the reflectivity profile is only sensitive to the interfacial monolayer, and with a D_2O subphase on which reflection is sensitive to the hydrogenous material.(36) The beam intensity was calibrated with respect to a clean D_2O surface.

Reflectivity data were fitted simultaneously using MOTOFIT(37), written for IGOR Pro, which uses the Abeles optical matrix method to calculate the reflectivity of

thin layers, each with a thickness, t; its corresponding SLD, ρ; a percentage hydration (% volume fraction of water) and a term for the roughness between layers, σ. It enables the global fitting of data sets of different isotopic compositions(37). A two-layer model was used to fit the data, where the upper layer (from the air to the subphase) represents the lipid tails and the lower layer corresponds to the polar headgroups.

It is well known in literature that under compression the molecular volumes of the methylene groups in the phospholipid chains reduces from LE to LC phases(38, 39). Campbell *et al*, have shown that the compaction of acyl chains with respect to their phase needs to be taken into account in the modeling of NR data at the air/water interface.(40) Thus, the SLD values (Table 1) used for modeling the neutron reflectivity data in this work, takes into account the compaction of the acyl chains with respect to their phase on h/d_{62}-DPPC as well as on the mixed monolayers. The antibiotics SLD values were calculated using the Molinspiration molecular properties calculator (http://www.molinspiration.com/cgi-bin/properties). For the mixed lipid-drug systems, the SLD of each layer was allowed to change under the constraint of a proper lipid/drug ratio (*i.e.*, 9:1 at 10% w/w of drug) either in the headgroup layer or the acyl tail layer, as follows:

$$\rho_{\text{Layer}} = \rho_{\text{DPPCtails}} * 0.9 + \rho_{\text{antibiotic}} * 0.1$$

This approach provides information related to the co-localization of the antibiotics within the DPPC monolayer.

Brewster angle microscopy

Lipid monolayers in the BAM experiments were prepared under the same conditions as described before. During the imaging procedure, BAM images were recorded periodically throughout continuous compression, using a Nima trough coupled with an ultra-objective BAM 2 Plus microscope (Nano Film EP4 Technology, Germany) connected to a high quality GigE CCD camera and appropriate 480 nm laser. The monolayer morphology was evaluated by inspecting the image: darker regions with no light reflection, result from a clean water surface or lower density lipid coverage, while the brighter spots correspond to dense monolayer domains(41)·(42).

Table 1. Summary of the fitting parameters used in the reflectivity calculations.

Lipid/antibiotic/subphase	$\rho/10^{-6}$ Å^{-2}	$\rho/10^{-6}$ Å^{-2} with 10% w/w of Levofloxacin	$\rho/10^{-6}$ Å^{-2} with 10% w/w of Clarithromycin
DPPC headgroup	1.75	1.75	1.75
h-DPPC tail	-0.36 (LE-phase) -0.42 (LC-phase)	-0.34 (LE-phase) -0.39 (LC-phase)	-0.33(LE-phase) -0.38 (LC-phase)
d-DPPC tail	6.87 (LE-phase) 7.94 (LC-phase)	6.35 (LE-phase) 7.32 (LC-phase)	6.25 (LE-phase) 7.21 (LC-phase)
Clarithromycin	0.66	-	-
Levofloxacin	1.7	-	-
D_2O	6.35	-	-
ACMW	0	-	-

Polarization-modulation infrared reflection absorption spectroscopy

PM-IRRAS measurements were taken with a KSV PMI 550 instrument (KSV instruments Ltd., Helsinki, Finland). The Langmuir trough is placed in a way that the light beam reaches the monolayer at a fixed incidence angle of 80°, at which the intensity is maximum with a low level of noise. The incoming light is continuously modulated between *s*- and *p*-polarization at a high frequency, which allows for the simultaneous measurement of the spectra for the two polarizations. The reflectivities for *s*- and *p*-polarizations, R_s and R_p, are acquired in the 800-4000 cm^{-1} range with 8 cm^{-1} resolution, and the differential spectrum is obtained by calculating the $(R_p-R_s)/(R_p+R_s)$ ratio(42)·(43)·

Results and discussion

The antibiotics Clarithromycin and Levofloxacin are not surface active and do not form Langmuir monolayers on their own. They do interact with DPPC monolayers at the air/water interface, as shown in the π-A isotherms in Figures 2A and 2C. The isotherms were repeated several times, and were shown to be reproducible. As expected for DPPC, the isotherm displays a plateau around ~8 mNm^{-1} characteristic of a LE (liquid expanded) – LC (liquid condensed) phase transition. Upon further compression, there was a steep change in slope of the isotherm reaching the LC phase with an area per molecule of ~46.2 Å^2 (at a surface pressure of 30 mNm^{-1}) also consistent with the literature(44)·(45). For mixed DPPC/Clarithromycin systems, there is a concentration dependent effect, since the addition of the drug shifts the isotherm to lower areas, i.e., causes monolayer condensation. The shift to lower areas is probably due to the change in surface

compressibility induced by Clarithromycin penetration into the monolayer, as seen in the change in slope of the isotherm in the LC region. Figures 2B and 2D show the surface compressional modulus, Cs^{-1}, as function of the surface pressure for the pure and mixed lipid-drug monolayers. Typical experimental values in the literature of surface compressional modulus for DPPC monolayers are 10–50 mNm^{-1} for LE films, 100–250 mNm^{-1} for LC films, and >250 mNm^{-1} for solid films(35)·(44). For the pure DPPC monolayer, the Cs^{-1} plot shows that above ca. 17 mNm^{-1} the lipid film is in a LC phase. However, for mixed DPPC/Clarithromycin systems, there is a slight depletion of Cs^{-1} values at the same surface pressure, and LC phases are reached only upon further lateral compression of the monolayer. It means that mixed DPPC/Clarithromycin monolayers became more compressible than the pure DPPC one. These results suggest a lipophilic interaction between Clarithromycin and the phospholipid tails, in addition to drug insertion into the film, which appears to be homogeneous according to the BAM images to be shown later on(46).

Figure 2. (A) Surface pressure-area (π-A) isotherms of pure (black) and mixed DPPC/Clarithromycin

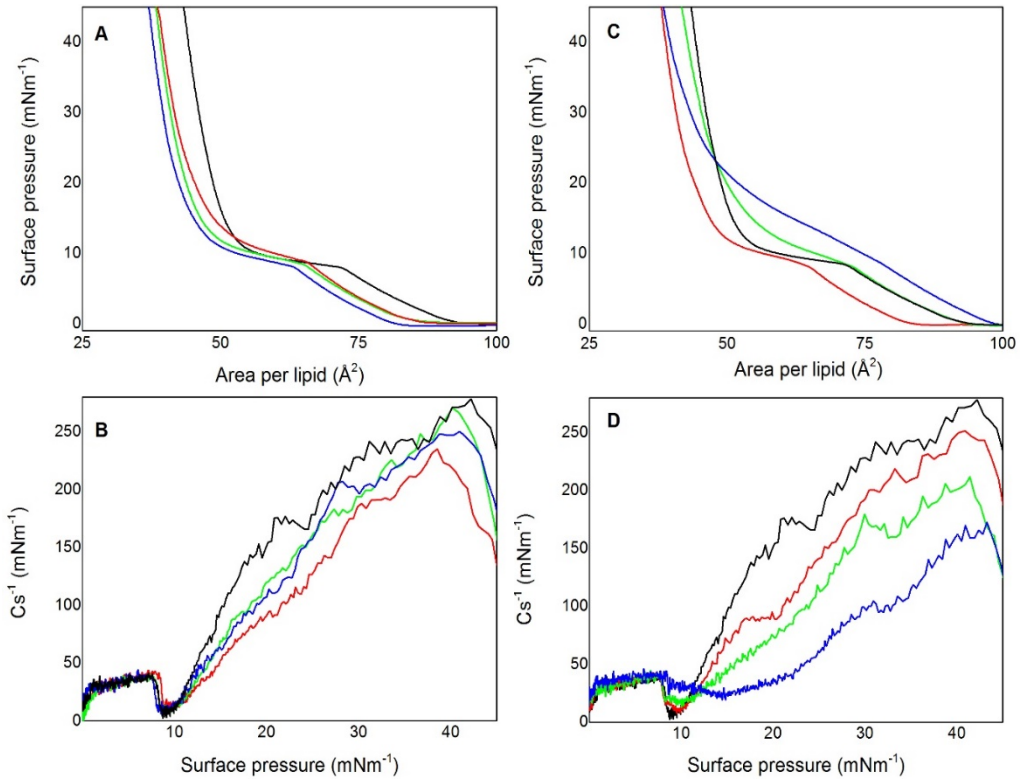

monolayers at 10 % w/w (blue); 1 % (green) and 0.1 % (red). (B) surface compressional modulus at the air-water interface calculated from the isotherms in (A). (C) Surface pressure-area (π-A) isotherms of pure DPPC (black) and mixed DPPC/Levofloxacin at 10 % w/w (blue); 1 % (green) and 0.1 % (red). (D) surface compressional modulus at the air-water interface from the isotherms in (B).

For mixed DPPC/Levofloxacin monolayer systems in Figure 2C, upon 0.1 % w/w Levofloxacin addition, a shift to lower areas in the isotherm was also observed. As the Levofloxacin concentration is increased, the isotherm profile displays a significant and increasing smoothness of the LE-LC phase transition plateau as well as changes in the slope of the isotherm at high surface pressures. It indicates changes in the packing of lipid molecules as well as a delay in the lateral monolayer organization. Regarding the monolayer elasticity in Figure 2D, there is a progressive increase of monolayer compressibility as Cs^{-1} values dramatically decrease to values below those for pure DPPC. Also, the delay in the LC phase formation is evident in Cs^{-1} plots, especially at high Levofloxacin concentration (10% w/w), since the monolayer remains at the LE state until high surface pressures (~30 mNm^{-1}) where it passes to the LC phase. The latter may be related to a different organization of the lipid molecules in the presence of a high drug concentration, which hinders the formation of the LC phase. Overall, these results could indicate that Levofloxacin interacts with phosphatidylcholine mainly through electrostatic interactions with the hydrophilic groups(47) and induces more elastic states, hence more compressible monolayers(48) than pure DPPC and DPPC/Clarithromycin mixtures. The collapse pressure of pure DPPC was around 68.7 mNm^{-1}, and this was not reduced with the addition of both drugs. Therefore, incorporation of both antibiotics does not affect or anticipate the normal phase transition process of DPPC monolayers.

Interfacial rheology experiments (see Figure S1 in the Supplementary material) on pure DPPC and mixed DPPC/antibiotics monolayers were also carried out using a double wall ring (DWR) geometry accessory in combination with a magnetic bearing stress rheometer (Discovery HR-3, TA Instruments, USA) on the dispersed films into the rheometer trough. As described in the previous Langmuir trough studies, the same stock solutions have been used here over an ultrapure water subphase. An oscillatory strain experiment showed that the surface shear modulus G' and G" of pure DPPC were indistinguishable from a clean water surface. However, an amplitude sweep test of the DPPC/antibiotic mixtures at the higher concentrations (Levofloxacin and Clarithromycin at 10% w/w) showed that the viscous modulus G" rose above noise level (Figure S1). The effect was more pronounced in the clarithromycin mixture than in the Levofloxacin one. Nevertheless, the flow curve and the frequency sweep tests just display noise. These results indicate that the addition of antibiotics affects the mechanical properties of the DPPC monolayer but they are not strong enough effects to be measured with the DWR

geometry. The fact that the viscous/loss moduli G" in the DPPC/Clarithromycin mixtures was higher than in the DPPC/Levofloxacin mixed monolayer demonstrates that the first one is a more viscous and ordered monolayer. Those results are in agreement with the surface compressional modulus Cs^{-1} results calculated from the π-A isotherms.

Figure 3 shows a summary of the BAM images recorded from π-A isotherms at 0 and 30 mNm^{-1} where the existence of lateral structural changes on the DPPC monolayer in the presence of both antibiotics is confirmed. Tables S1 and S2 in the Supplementary material present the full images of pure and mixed DPPC/Levofloxacin and DPPC/Clarithromycin monolayers recorded as a function of surface pressure. Ordered condensed domains of pure DPPC are formed at very low surface pressure in the form of small patches (~ 5 mNm^{-1}) that grow in size and gain a lobulated shape under lateral compression (typical for the enantiomeric DPPC molecule(49)). These DPPC domains achieve high molecular packing and become a LC phase at surface pressures between 20 and 30 mNm^{-1}. With the increase of Levofloxacin and Clarithromycin concentrations, the lipid domains adopt a more star-like shape due to their interaction with antibiotic molecules. Previous reports(50, 51) attribute changes in the shape of DPPC domains to the presence of particles that modify the line tension between domains, which affect their appearance. Moreover, the LC phase is reached at smaller surface areas (for the same pressure), indicating the loss of molecular arrangement, as reflected by the black holes (defects) at surface pressures > 30 mNm^{-1}. When the antibiotic content is higher than 1%, bright circular domains are observed, which may indicate the existence of lipid/drug aggregates which have a lower line tension than pure DPPC domains. These aggregates affect the DPPC molecular organization, thus changing the isotherms as in Figure 2.

Figure 4 compares the PM-IRRAS spectra of pure DPPC with the addition of Clarithromycin and Levofloxacin at 0.1 and 10% (w/w) and a surface pressure of 30 mNm^{-1} in the headgroup region. Pure DPPC bands at 1698 cm^{-1} (C=O stretching, fatty acid) and 1742 cm^{-1} (C=O stretching, ester) change their orientation (downwards to upwards) with increasing surface pressure, indicating that phospholipids headgroups change their orientation from perpendicular to parallel to the air-water interface upon compression as can be seen in Figure S2 A. With the addition of Clarithromycin and Levofloxacin at any studied quantity, the polar phospholipid headgroups are no longer sensitive to surface pressure, remaining with the same orientation (parallel). This is an indication that both antibiotics have interaction with the phospholipid headgroups.

Furthermore, no significant changes were observed for alkyl tail bands at 2850 cm^{-1} (CH_2 symmetric) and 2925 cm^{-1} (CH_2 antisymmetric) (Figure S2 C-J). The PM-IRRAS spectra indicate that clarithromycin and levofloxacin interact with the headgroups of DPPC. Also, they affect the organization of DPPC upon compression. The bands centered at 1650 and 1547 cm^{-1} represents the effect of interfacial water molecules, and are usually attributed to the difference of reflectivities of the air–water interface covered and uncovered by the monolayer(52, 53).

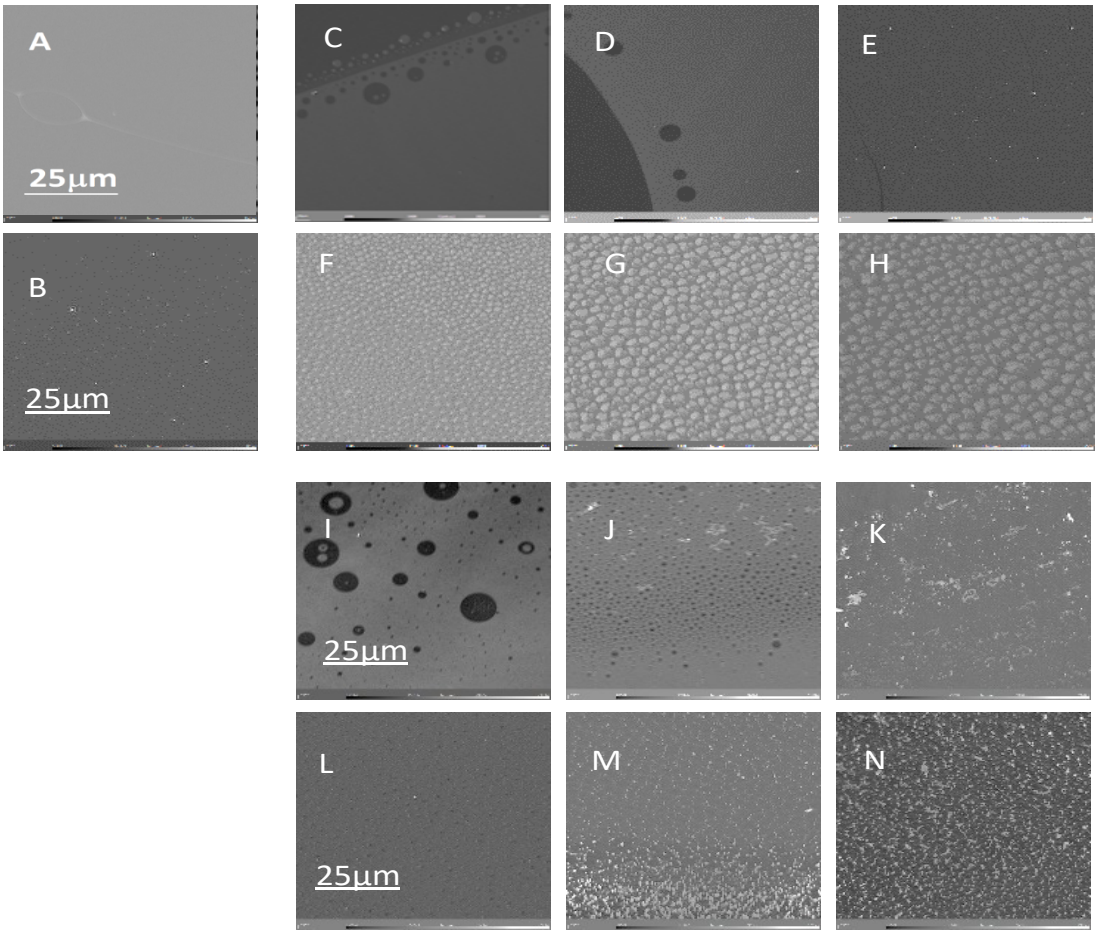

Figure 3. Brewster angle microscopy images of pure DPPC (1 $g.L^{-1}$) (A) 0 mNm^{-1} and (B) 30 mNm^{-1}. Mixed DPPC/Clarithromycin at 0 mNm^{-1} (C 0.1% w/w; D 1%; E 10%) and 30 mNm^{-1} (F 0.1% w/w; G 1%; H 10%). Mixed DPPC/Levofloxacin at 0 mNm^{-1} (I 0.1% w/w; J 1%; K 10%) and 30 mNm^{-1} (L 0.1% w/w; M 1%; N 10%). All BAM images have a 25 µm scale bar at the left hand corner.

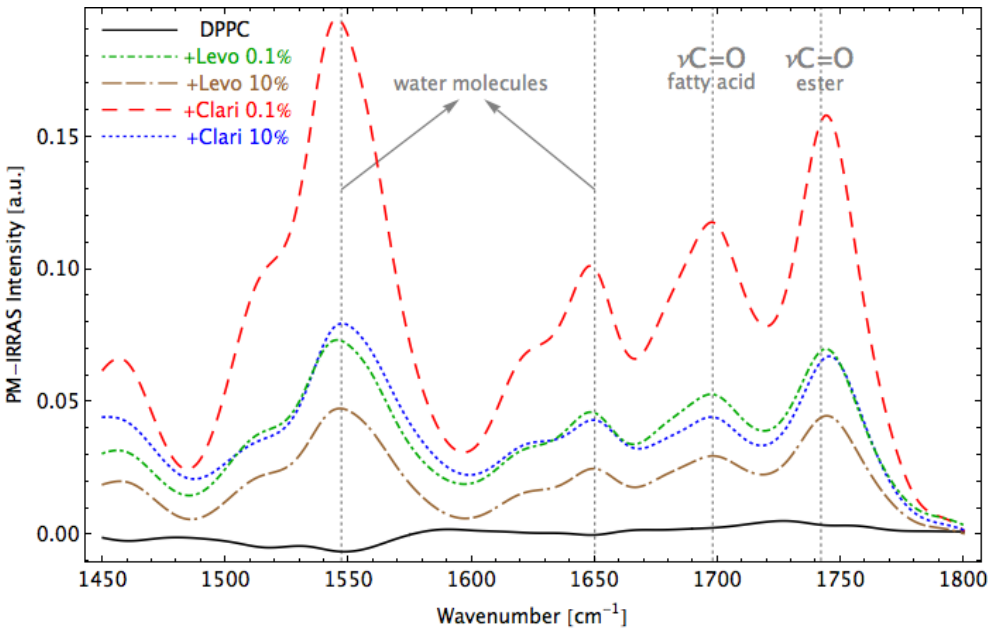

Figure 4. Experimental PM-IRRAS spectra of Langmuir films of pure DPPC (black solid line), DPPC/Levofloxacin 0.1% w/w (green dot-dashed line), DPPC/levofloxacin 10% w/w (brown double-dashed-dot line), DPPC/ Clarithromycin 0.1% w/w (red dashed line) and DPPC/ Clarithromycin 10% w/w (blue dot line) at the head groups region (1450–1800 cm^{-1}) and a surface pressure of 30 mNm^{-1}.

Before NR studies, the stability of the mixed monolayers was checked by holding the target surface pressures using a feedback loop. All the systems were left undisturbed for a lapse of time of 90 min with little loss of material from the interface (less than ~5% in area). Two reflectometry profiles for a pure DPPC monolayer over different subphases: D_2O and ACMW, along with their corresponding SLD profile at 30 mNm^{-1} are presented in Figure 5. Simultaneous two-layer model fitting of the experimental reflectometry data revealed that our results are consistent with published results(45). Table 2 lists the structural parameters used in the fitting procedure for h-DPPC/d_{62}-DPPC. In the fitting of the different contrast data sets, the layer thicknesses were constrained between each data set, because it is assumed that the physical dimensions of the films are unaffected by changes in deuteration of the components(25). From the data sets it is possible to see the interfacial film emerging as the surface pressure increases and the reflectivity profiles display higher intensity. At a surface pressure of 30 mNm^{-1} these fittings provide an area per lipid molecule of 47.7 $Å^2$ (from the lipid tails) and a thickness of the hydrocarbon layer of 16.2 Å, resulting in a tilt angle (relative to surface normal) of 32.2° calculated as follows: $\beta=\arccos(t_{tails}/l_{palmitoyl})$. The length ($l$) of the DPPC tails used was 19.15 Å as

reported by Vaknin *et al*(54, 55), compatible with previous DPPC tilt angles reported(56–62).

Figures 6 and 7 show the NR profiles and the best data fitting for the mixed lipid-drug curves at 30 mN m^{-1}; as well as their corresponding SLD profiles for a concentration of 10 % w/w.

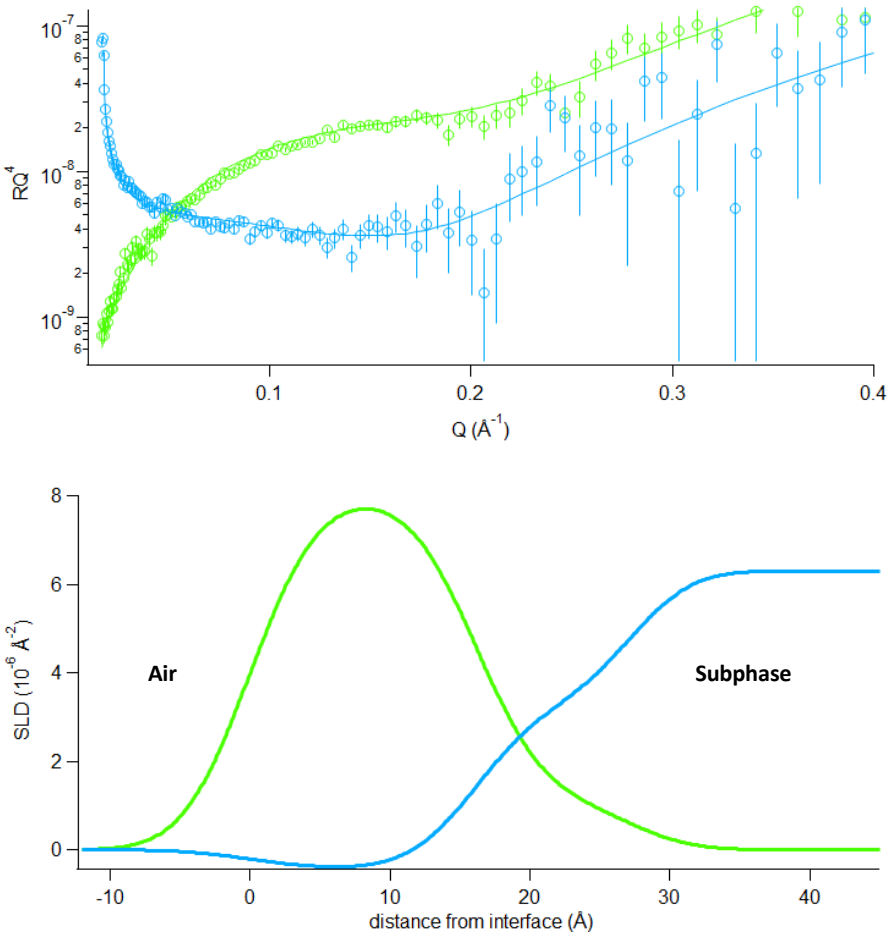

Figure 5. Neutron Reflectometry data and the best two-layer fittings from simultaneous fitted d-DPPC on ACMW (green) and h-DPPC on D_2O (blue) monolayers at the air-water interface and a surface pressure of 30 mNm^{-1}. Upper figure: Reflectivity vs Q ($Å^{-1}$), Lower figure: The scattering length density plot of all contrasts vs the distance from the interface.

Table 2. Fitting structural parameters for a pure DPPC monolayer using two isotopic contrasts at surface pressures of 5, 20 and 30 mNm^{-1}.

Layer	Contrast	Model: Surface pressure/mNm^{-1}									Area per lipid/ $Å^2$ (30 mNm^{-1})	
		5			20			30			Exp.	Calc.
		t/Å	σ/Å	%Hyd	t/Å	σ/Å	%Hyd	t/Å	σ/Å	%Hyd		
1-Tails	h-DPPC on D_2O	11.0 ± 0.5	4.5 ± 0.2	-	15.5 ± 0.2	3.9 ± 0.3	-	16.2 ± 0.2	3.8 ± 0.3	-	46.2 ± 0.1	47.7 ± 0.1
	d-DPPC on ACMW										Alkyl tail tilt angle (relative to the surface normal)	
2-heads	h-DPPC on D_2O	11.6 ± 0.7	4.5 ± 0.3	63 ± 5	11.0 ± 0.6	3.8 ± 0.3	36 ± 4	11.0 ± 0.6	3.8 ± 0.2	35 ± 5	32.2°	
	d-DPPC on ACMW											

Table 3. Fitting structural parameters for a DPPC/Clarithromycin (CLA) monolayer using three isotopic contrasts at surface pressures of 5, 20 and 30mN m^{-1}. θ is the alkyl tail tilt angle relative to the surface normal.

Layer	Contrast: d-DPPC on D_2O or ACMW h-DPPC on D_2O	Model: Surface pressure/mNm^{-1}									Area per lipid/ $Å^2$ (30 mNm^{-1})		θ (°)
		5			20			30			Exp.	Calc.	
		t/Å	*σ*/Å	%Hyd	*t*/Å	*σ*/Å	%Hyd	*t*/Å	*σ*/Å	%Hyd			
1-Tails	CLA/DPPC 0.1 %	11.5 ± 0.1	5.9 ± 0.3	-	15.5 ± 0.1	5.6 ± 0.2	-	17.0 ± 0.1	5.3 ± 0.2	-	41.6 ± 0.1	45.4 ± 0.1	27.4
2-Heads	CLA/DPPC 0.1 %	10.0 ± 0.5	5.5 ± 0.2	55 ± 2	11.5 ± 0.3	5.7 ± 0.2	38 ± 2	9.0 ± 0.4	5.3 ± 0.1	16 ± 1			
1-Tails	CLA/DPPC 1 %	11.5 ± 0.3	5.0 ± 0.4	-	15.5 ± 0.1	5.5 ± 0.6	-	17.3 ± 0.6	5.8 ± 0.3	-	40.9 ± 0.1	44.6 ± 0.1	25.4
2-Heads	CLA/DPPC 1 %	11.0 ± 0.5	5.0 ± 0.5	50 ± 3	11.0 ± 0.3	5.5 ± 0.7	30 ± 5	10.5 ± 0.4	5.5 ± 0.2	20 ± 3			
1-Tails	CLA/DPPC 10 %	13.5 ± 0.3	5.5 ± 0.2	-	17.5 ± 0.3	5.5 ± 0.4	-	19.0 ± 0.3	5.0 ± 0.2	-	39.6 ± 0.2	44.8 ± 0.1	7.2
2-Heads	CLA/DPPC 10 %	11.0 ± 0.5	5.5 ± 0.3	57 ± 3	10.0 ± 0.2	5.5 ± 0.3	30 ± 3	9.5 ± 0.4	5.0 ± 0.1	22 ± 4			

Table 4. Fitting structural parameters for a DPPC/Levofloxacin (LEV) monolayer using different isotopic contrasts at surface pressures of 5, 20 and 30mN m^{-1}. θ is the alkyl tail tilt angle relative to the surface normal.

Layer	Contrast: d-DPPC on D_2O or ACMW h-DPPC on D_2O	Model: Surface pressure/mNm^{-1}									Area per lipid/ $Å^2$ ($30mNm^{-1}$)		θ (°)
		5			20			30			Exp.	Calc.	
		t/Å	*σ*/Å	%Hyd	*t*/Å	*σ*/Å	%Hyd	*t*/Å	*σ*/Å	%Hyd			
1-Tails	LEV/DPPC 0.1 %	11.8 ± 0.4	5.5 ± 0.1	-	15.5 ± 0.4	5.5 ± 0.2	-	17.5 ± 0.1	5.3 ± 0.2	-	40.7 ± 0.1	44.1 ± 0.1	24.0
2-Heads	LEV/DPPC 0.1 %	11.5 ± 0.2	5.0 ± 0.1	60 ± 3	9.5 ± 0.5	5.5 ± 0.3	20 ± 3	10.0 ± 0.2	5.0 ± 0.5	21 ± 2			
1-Tails	LEV/DPPC 1 %	10.5 ± 0.4	5.3 ± 0.5	-	14.0 ± 0.6	5.0 ± 0.5	-	15.5 ± 0.5	3.5 ± 0.3	-	45.0 ± 0.3	49.8 ± 0.1	36.0
2-Heads	LEV/DPPC 1 %	11.0 ± 0.5	5.5 ± 0.3	60 ± 4	11.0 ± 0.5	5.0 ± 0.4	30 ± 2	11.0 ± 0.4	4.0 ± 0.5	28 ± 2			
1-Tails	LEV/DPPC 10 %	10.5 ± 0.5	5.5 ± 0.5	-	15.0 ± 0.5	4.5 ± 0.3	-	17.5 ± 0.2	5.0 ± 0.3	-	43.2 ± 0.3	47.7 ± 0.1	24.0
2-Heads	LEV/DPPC 10 %	11.0 ± 0.3	5.2 ± 0.2	62 ± 2	12.0 ± 0.4	5.0 ± 0.3	40 ± 5	12.0 ± 0.4	4.5 ± 0.4	40 ± 3			

The influence from both antibiotics on the interfacial structure of DPPC monolayers is seen in the structural parameters in Tables 3 and 4. The best fits for mixed DPPC/Clarithromycin monolayers were obtained considering that the molecule is located within the hydrocarbon tails. The introduction of Clarithromycin showed a thickness increase of the tail groups from 16.2 to 19.0 Å (at 30 mNm^{-1} and 10% of drug) and increased roughness from 3.8 to 5.0 Å at the top of the tails. These effects are in agreement with the Clarithromycin compressional effect in the monolayer, in consequence, the tilt angle of the tail decreases as the concentration of drug increases(25),(63). On the other hand, there was also a decrease in the solvent penetration of the headgroups, from ~ 35% in pure DPPC monolayers to 22% at the highest addition of drug; as well as a smooth reduction in the headgroup thickness (from ~ 11.0 to 9.5 Å). From Kosol *et al*(64), it is known that macrolides are able to bind to membrane models through electrostatic interactions between the amino groups of the macrolides with the phospholipid headgroup. Clarithromycin, chemically known as 6-O-methylerythromycin A, contains in its structure a desosamine ring (deoxy sugar), permitting it to exist in both protonated (>96%) and neutral (<4%) forms at physiological pH due to the pKa of the dimethylamino group (~8.6-8.9)(65, 66). These results indicate that Clarithromycin, owing to its hydrophobic nature, co-localizes mainly within the acyl tails of DPPC through van der Waals forces(67). Furthermore, Clarithromycin probably guides its deoxy sugar units close to the polar headgroups allowing the positively charged amino group to interact with the polarizable PC headgroups.

From the best data fits of Levofloxacin mixtures, (which differs from Clarithromycin due to its hydrophilic character and its smaller volume), it was possible to observe a less remarkable increase in the tail thickness along with a reduction in its tilt angle (from ~16.2 to 17.5 Å and ~ 32.2° to 24° respectively) according to the compressional effect of the drug in the monolayer. Earlier studies have indicate the ability of a fluoroquinolone antibiotic (Ciprofloxacin) to slightly alter the tilt angle of the acyl chain of DPPC monolayers(24, 68). In addition, it was noticed that Levofloxacin induces an increase in the headgroups thickness from ~11 to 12 Å. Also, the hydration percentage of the headgroups was reduced at low Levofloxacin concentration but it increases from 35% to 40% at the highest addition of drug. These results suggest that Levofloxacin, as a zwitterionic molecule at pH ~ 7 (69–71), penetrates the monolayer and co-localizes mainly at the head to tail interfacial region. Since fluoroquinolones enable attractive

interplays between the positively charged piperazine ring at the C-7 position of the quinolone and the negatively charged phosphate groups of the phospholipid heads(47, 72, 73) , Levofloxacin could replace water molecules surrounding the headgroup region through electrostatic dipole-dipole interactions (hydrogen-bond interactions). This could explain the differences found in the SLD profile format in the headgroup region at 30 mNm^{-1}, compared with the pure DPPC SLD profile. These observed effects are consistent with a decreased area per lipid molecule seen in the surface pressure isotherms. In the paper Ortiz-Collazos, *et al*(9), have been shown by MD simulations that Levofloxacin molecules are located preferentially between the polar head groups phospholipids at surface pressures of 43 mNm^{-1} which is in agreement with the results presented here.

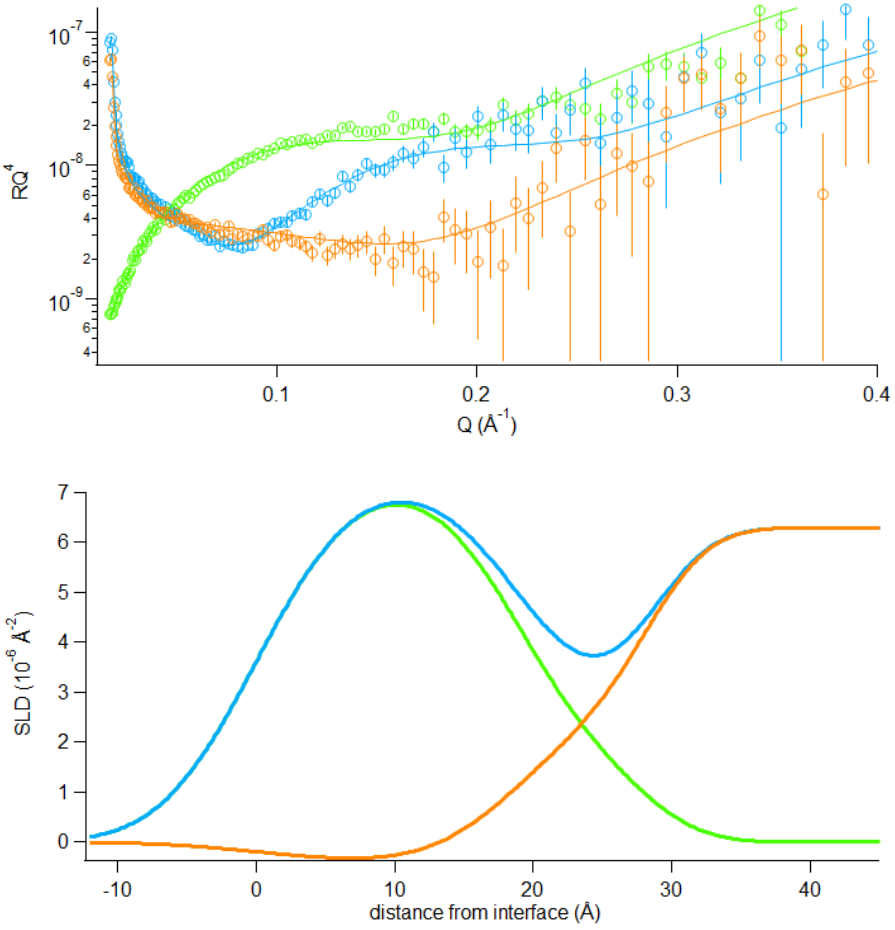

Figure 6. Neutron Reflectometry data and the best two-layer fittings obtained from simultaneous fitted h-DPPC/Clarithromycin on D_2O (orange); d-DPPC/Clarithromycin on D_2O (blue) and d-DPPC/Clarithromycin on ACMW (green) 10% w/w monolayers at the air-water interface and surface pressure of 30 mNm^{-1}. Upper Figure: Reflectivity vs Q ($Å^{-1}$). Lower Figure: The scattering length density plot of all contrasts vs the distance from the interface.

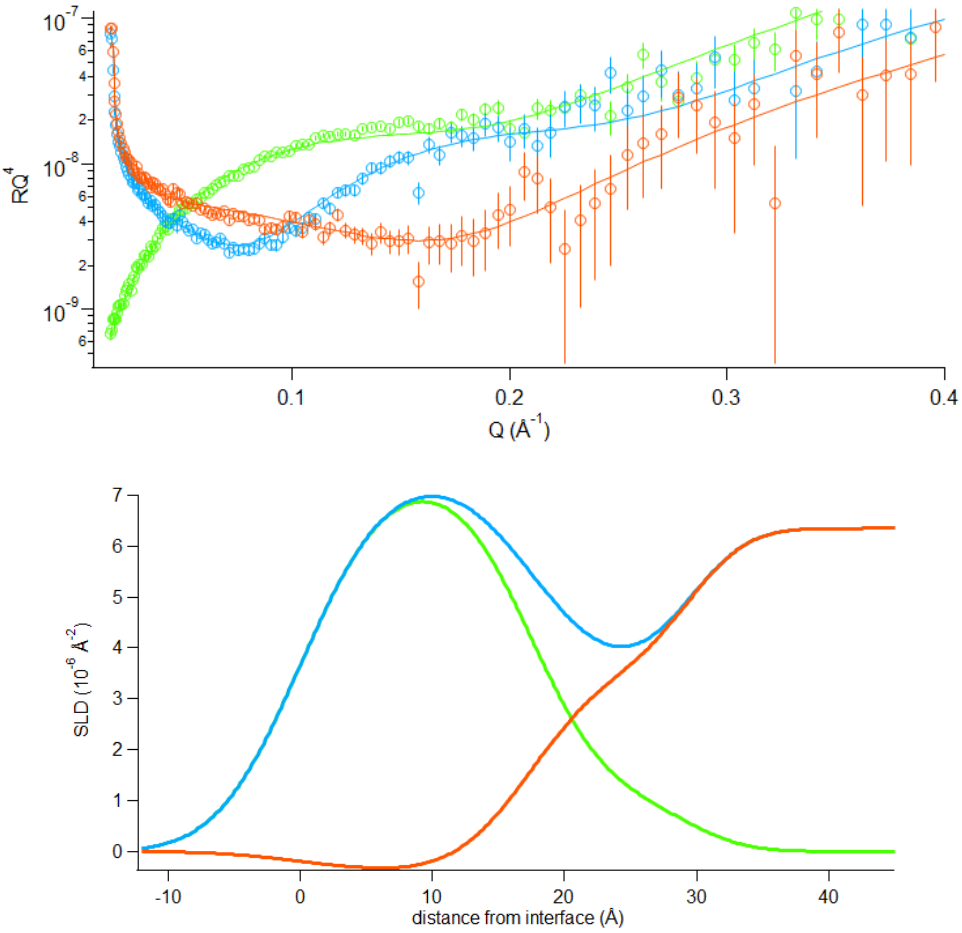

Figure 7. Neutron Reflectometry data and the best two-layer fittings from simultaneous fitted h-DPPC/Levofloxacin on D_2O (orange); d-DPPC/Levofloxacin on D_2O (blue) and d-DPPC/Levofloxacin on ACMW (green) 10% w/w monolayers at the air-water interface and a surface pressure of 30 mNm^{-1}. Upper Figure: Reflectivity vs Q ($Å^{-1}$), Lower Figure: The scattering length density plot of all contrasts vs the distance from the interface.

Our results show that the effects of introducing both drugs on DPPC monolayers are related with the particularities of their interplay with the lipid membrane model. The lower compressibility values found in Levofloxacin mixtures, especially at 10% w/w and 30 mNm^{-1}, indicates a high fluidity of the model membrane at this point. This fact, as well as the Levofloxacin preferential interaction with polar headgroups, may directly affect the drug diffusion at the surface packing pressure found in biological membranes (~ 30-35 mNm^{-1})(74). On the other hand, Clarithromycin due to its high lipophilicity is inserted within the lipid tails inducing perturbations on the monolayer organization. These interactions could modulate a high accumulation of the antibiotic at the membrane along with a slow release to an aqueous phase(67). Also, this could have a direct impact on

reduced bacterial biofilm growth at the airway epithelium. The structural information obtained about the orientation and localization of the antibiotics in the lung surfactant membrane-mimetic system facilitates the understanding of the interaction of such compounds with lipid membranes to predict the biophysical behavior of future smart drug-delivery formulations.

Conclusions

From this information, we have determined the structural details of the interaction between Levofloxacin and Clarithromycin antibiotics, each interacting with DPPC monolayers respectively. Langmuir studies shown that the introduction of both antibiotics induces changes in packing and lipid organization, as evidenced by a shifting in the isotherm to lower areas i.e., causing the monolayers to be more compressible. BAM experiments confirmed changes in the DPPC domains structure in the presence of the antibiotics which modify its molecular arrangement. The effects of the antibiotics differ due to their different physicochemical natures modifying the elastic properties of DPPC monolayers. NR data analysis showed that Clarithromycin, as a bulky hydrophobic molecule, merged into the hydrocarbon tails region allowing its deoxy sugar units to be close to the polar headgroups. Clarithromycin is able to induce a considerable reduction in the tilt angle of the lipid tails as well as reducing the thickness and solvent penetration of the polar headgroups. On the other hand, the smaller Levofloxacin produces a larger effect on the isotherm profile at high drug concentration (10% w/w), causing a delay in the LE-LC phase transition, hinders the phospholipid molecular organization, and induces a considerable decrease in the compressional modulus. The NR results indicate that Levofloxacin co-localizes mainly affecting the polar headgroups since it slightly increases both tail and head groups thickness as well as reduces the solvent penetration of the polar region and the acyl tail tilt. The presence of both antibiotics also induces the roughening at the head and the tail region of the mixed monolayers, when compared with pure DPPC monolayers, which confirms their insertion. These effects corroborate changes in the packing and the lateral organization of the DPPC molecules, as well as the integration of these antibiotics into the monolayer. Further, the stability, functionality and the 2D to 3D transition process in the DPPC monolayer (‘collapse mechanism’), was not compromised at any drug concentration studied. We believe that this work can contribute to a better understanding and control of the molecular basis related to the interaction of

theses antibiotics with lung surfactant models and thus, in the design of new strategies in respiratory medicine.

Author Contributions

SOC designed research, performed research, analyzed data, and wrote the manuscript.

PHSP performed research and analyzed data.

ONO contributed with analytical tools, analyzed data, and wrote the manuscript.

ASP designed research, analyzed data, and wrote the manuscript

KJE designed research, contributed with analytical tools, analyzed data, and wrote the manuscript.

Acknowledgements

The authors are grateful to FAPERJ (Grant No. 210.558/2015, and E-26/010.001241/2016), the National Council for Scientific and Technological Development (CNPq, Grant No. 465259/2014-6), the National Institute of Science and Technology Complex Fluids (INCT-FCx), and the São Paulo Research Foundation (FAPESP, Grant No. 2014/50983-3, 2013/14262-7 and 210.558/2015). SOC is thankful to CAPES for a sandwich doctorate scholarship (No.88881.132891/2016-01). We acknowledge Dr. Cristiano R. W. Magalhães (Aché Laboratórios Farmacêuticos), who supplied the antibiotics active samples. We would also like to thank ISIS Pulsed Neutron and Muon source for the beamtime (experiment number RB1710178) and the SURF beamline staff for their assistance in collecting the NR data. Thanks are also extended to the Edler research group from the University of Bath for their assistance in developing this work.

References

1. Hermans, E., M. Saad Bhamla, P. Kao, G.G. Fuller, and J. Vermant. 2015. Lung surfactants and different contributions to thin film stability. Soft Matter. 11: 8048–8057.

2. Parra, E., and J. Pérez-Gil. 2015. Composition, structure and mechanical properties define performance of pulmonary surfactant membranes and films. Chem. Phys. Lipids. 185: 153–75.

3. Pérez-Gil, J. 2008. Structure of pulmonary surfactant membranes and films: The role of proteins and lipid-protein interactions. Biochim. Biophys. Acta - Biomembr. 1778: 1676–1695.

4. Haitsma, J. 2001. Exogenous surfactant as a drug delivery agent. Adv. Drug Deliv. Rev. 47: 197–207.

5. Duan, J., F.G. Vogt, X. Li, D. Hayes, and H.M. Mansour. 2013. Design, characterization, and aerosolization of organic solution advanced spray-dried moxifloxacin and ofloxacin dipalmitoylphosphatidylcholine (DPPC) microparticulate/nanoparticulate powders for pulmonary inhalation aerosol delivery. Int. J. Nanomedicine. 8: 3489–3505.

6. Brezesinski, G., and H. Möhwald. 2003. Langmuir monolayers to study interactions at model membrane surfaces. Adv. Colloid Interface Sci. 100–102: 563–584.

7. Deleu, M., M. Paquot, and T. Nylander. 2005. Fengycin interaction with lipid monolayers at the air-aqueous interface - Implications for the effect of fengycin on biological membranes. J. Colloid Interface Sci. 283: 358–365.

8. Griffith, E.C., T.R.C. Guizado, A.S. Pimentel, G.S. Tyndall, and V. Vaida. 2013. Oxidized aromatic-aliphatic mixed films at the air-aqueous solution interface. J. Phys. Chem. C. 117: 22341–22350.

9. Ortiz-Collazos, S., E.D. Estrada-López, A.A. Pedreira, P.H.S. Picciani, O.N. Oliveira, and A.S. Pimentel. 2017. Interaction of levofloxacin with lung surfactant at the air-water interface. Colloids Surfaces B Biointerfaces. 158: 689–696.

10. Ortiz-Collazos, S., Y.M.H. Gonçalves, B.A.C. Horta, P.H.S. Picciani, S.R.W.

Louro, O.N. Oliveira, and A.S. Pimentel. 2016. Langmuir films and mechanical properties of polyethyleneglycol fatty acid esters at the air-water interface. Colloids Surfaces A Physicochem. Eng. Asp. 498: 50–57.

11. Pantoja-Romero, W.S., E.D. Estrada-López, P.H.S. Picciani, O.N. Oliveira, E.R. Lachter, and A.S. Pimentel. 2016. Efficient molecular packing of glycerol monostearate in Langmuir monolayers at the air-water interface. Colloids Surfaces A Physicochem. Eng. Asp. 508: 85–92.

12. Hac-Wydro, K., and P. Dynarowicz-Łatka. 2006. Nystatin in Langmuir monolayers at the air/water interface. Colloids Surfaces B Biointerfaces. 53: 64–71.

13. Jabłonowska, E., and R. Bilewicz. 2007. Interactions of ibuprofen with Langmuir monolayers of membrane lipids. Thin Solid Films. 515: 3962–3966.

14. Jyoti, A., R.M. Prokop, J. Li, D. Vollhardt, D.Y. Kwok, R. Miller, H. Möhwald, and A.W. Neumann. 1996. An investigation of the compression rate dependence on the surface pressure-surface area isotherm for a dipalmitoyl phosphatidylcholine monolayer at the air/water interface. Colloids Surfaces A Physicochem. Eng. Asp. 116: 173–180.

15. Weidemann, G., and D. Vollhardt. 1995. Long range tilt orientational order in phospholipid monolayers: a comparison of the order in the condensed phases of dimyristoylphosphatidylethanolamine and dipalmitoylphosphatidylcholine. Colloids Surfaces A Physicochem. Eng. Asp. 100: 187–202.

16. Hidalgo, A.A., A.S. Pimentel, M. Tabak, and O.N. Oliveira. 2006. Thermodynamic and infrared analyses of the interaction of chlorpromazine with phospholipid monolayers. J. Phys. Chem. B. 110: 19637–19646.

17. Pérez, S., J. Miñones, M. Espina, M.A. Alsina, I. Haro, and C. Mestres. 2005. Influence of the saturation chain and head group charge of phospholipids in the interaction of hepatitis G virus synthetic peptides. J. Phys. Chem. B. 109: 19970–19979.

18. Padilla-Chavarría, H.I., T.R.C. Guizado, and A.S. Pimentel. 2015. Molecular dynamics of dibenz[a,h]anthracene and its metabolite interacting with lung surfactant phospholipid bilayers. Phys. Chem. Chem. Phys. 17: 20912–20922.

19. Estrada-López, E.D., E. Murce, M.P.P. Franca, and A.S. Pimentel. 2017. Prednisolone adsorption on lung surfactant models: Insights on the formation of nanoaggregates, monolayer collapse and prednisolone spreading. RSC Adv. 7: 5272–5281.

20. Souza, L.M.P., J.B. Nascimento, A.L. Romeu, E.D. Estrada-López, and A.S. Pimentel. 2018. Penetration of antimicrobial peptides in a lung surfactant model. Colloids Surfaces B Biointerfaces. 167: 345–353.

21. Di Cola, E., I. Grillo, and S. Ristori. 2016. Small angle X-ray and neutron scattering: Powerful tools for studying the structure of drug-loaded liposomes. Pharmaceutics. 8: 1–16.

22. Kiselev, M.A. 2011. Methods for lipid nanostructure investigation at neutron and synchrotron sources. Phys. Part. Nucl. 42: 302–331.

23. Pinheiro, M., J.J. Giner-Casares, M. Lúcio, J.M. Caio, C. Moiteiro, J.L.F.C. Lima, S. Reis, and L. Camacho. 2013. Interplay of mycolic acids, antimycobacterial compounds and pulmonary surfactant membrane: A biophysical approach to disease. Biochim. Biophys. Acta - Biomembr. 1828: 896–905.

24. Bensikaddour, H., N. Fa, I. Burton, M. Deleu, L. Lins, A. Schanck, R. Brasseur, Y.F. Dufrêne, E. Goormaghtigh, and M.-P. Mingeot-Leclercq. 2008. Characterization of the Interactions between Fluoroquinolone Antibiotics and Lipids: a Multitechnique Approach. Biophys. J. 94: 3035–3046.

25. Fullagar, W.K., S. a Holt, and I.R. Gentle. 2008. Structure of SP-B/DPPC mixed films studied by neutron reflectometry. Biophys. J. 95: 4829–36.

26. Follows, D., F. Tiberg, R.K. Thomas, and M. Larsson. 2007. Multilayers at the surface of solutions of exogenous lung surfactant: Direct observation by neutron reflection. Biochim. Biophys. Acta - Biomembr. 1768: 228–235.

27. Duan, J., F.G. Vogt, X. Li, D. Hayes, and H.M. Mansour. 2013. Design, characterization, and aerosolization of organic solution advanced spray-dried moxifloxacin and ofloxacin dipalmitoylphosphatidylcholine (DPPC) microparticulate/nanoparticulate powders for pulmonary inhalation aerosol delivery. Int. J. Nanomedicine. 8: 3489–3505.

28. Michel, J.P., Y.X. Wang, I. Kiesel, Y. Gerelli, and V. Rosilio. 2017. Disruption of Asymmetric Lipid Bilayer Models Mimicking the Outer Membrane of Gram-Negative Bacteria by an Active Plasticin. Langmuir. 33: 11028–11039.

29. Clifton, L.A., M.W.A. Skoda, E.L. Daulton, A. V. Hughes, A.P. Le Brun, J.H. Lakey, and S.A. Holt. 2013. Asymmetric phospholipid: lipopolysaccharide bilayers; a Gram-negative bacterial outer membrane mimic. J. R. Soc. Interface. 10: 20130810–20130810.

30. Han, M.-L., H.-H. Shen, K.A. Hansford, E.K. Schneider, S. Sivanesan, K.D. Roberts, P.E. Thompson, A.P. Le Brun, Y. Zhu, M.-A. Sani, F. Separovic, M.A.T. Blaskovich, M.A. Baker, S.M. Moskowitz, M.A. Cooper, J. Li, and T. Velkov. 2017. Investigating the Interaction of Octapeptin A3 with Model Bacterial Membranes. ACS Infect. Dis. 3: 606–619.

31. Togami, K., S. Chono, and K. Morimoto. 2012. Aerosol-based efficient delivery of clarithromycin, a macrolide antimicrobial agent, to lung epithelial lining fluid and alveolar macrophages for treatment of respiratory infections. J. Aerosol Med. Pulm. Drug Deliv. 25: 110–5.

32. Davies, J.T., and E.K. Rideal. 1963. Interfacial phenomena. second ed. New York: Academic Press.

33. Penfold, J., R.M. Richardson, A. Zarbakhsh, J.R.P. Webster, D.G. Bucknall, A.R. Rennie, R.A.L. Jones, T. Cosgrove, R.K. Thomas, J.S. Higgins, P.D.I. Fletcher, E. Dickinson, S.J. Roser, I.A. McLure, A.R. Hillman, R.W. Richards, E.J. Staples, A.N. Burgess, E.A. Simister, and J.W. White. 1997. Recent advances in the study of chemical surfaces and interfaces by specular neutron reflection. J Chem Soc Faraday Trans. 93: 3899–3917.

34. Clifton, L.A., M.R. Sanders, A. V Hughes, C. Neylon, R.A. Frazier, and R.J. Green. 2011. Lipid binding interactions of antimicrobial plant seed defence proteins: puroindoline-a and beta-purothionin. Phys. Chem. Chem. Phys. 13: 17153–17162.

35. Hazell, G., A.P. Gee, T. Arnold, K.J. Edler, and S.E. Lewis. 2016. Langmuir monolayers composed of single and double tail sulfobetaine lipids. J. Colloid Interface Sci. 474: 190–198.

36. Clifton, L.A., M. Sanders, C. Kinane, T. Arnold, K.J. Edler, C. Neylon, R.J. Green, and R.A. Frazier. 2012. The role of protein hydrophobicity in thionin-phospholipid interactions: a comparison of α1 and α2-purothionin adsorbed anionic phospholipid monolayers. Phys. Chem. Chem. Phys. 14: 13569–79.

37. Nelson, A. 2006. Co-refinement of multiple-contrast neutron/X-ray reflectivity data using MOTOFIT. J. Appl. Crystallogr. 39: 273–276.

38. Marsh, D. 2010. Molecular volumes of phospholipids and glycolipids in membranes. Chem. Phys. Lipids. 163: 667–677.

39. McConlogue, C.W., and T.K. Vanderlick. 2002. A Close Look at Domain Formation in DPPC Monolayers. Langmuir. 13: 7158–7164.

40. Campbell, R.A., Y. Saaka, Y. Shao, Y. Gerelli, R. Cubitt, E. Nazaruk, D. Matyszewska, and M.J. Lawrence. 2018. Structure of surfactant and phospholipid monolayers at the air/water interface modeled from neutron reflectivity data. J. Colloid Interface Sci. 531: 98–108.

41. Geraldo, V.P.N., F.J. Pavinatto, T.M. Nobre, L. Caseli, and O.N. Oliveira. 2013. Langmuir films containing ibuprofen and phospholipids. Chem. Phys. Lett. 559: 99–106.

42. Pinheiro, M., M. Arêde, J.J. Giner-Casares, C. Nunes, J.M. Caio, C. Moiteiro, M. Lúcio, L. Camacho, and S. Reis. 2013. Effects of a novel antimycobacterial compound on the biophysical properties of a pulmonary surfactant model membrane. Int. J. Pharm. 450: 268–77.

43. Sandrino, B., T.T. Tominaga, T.M. Nobre, L. Scorsin, E.C. Wrobel, B.C. Fiorin, M.P. De Araujo, L. Caseli, O.N. Oliveira, and K. Wohnrath. 2014. Correlation of [RuCl<inf>3</inf>(dppb)(VPy)] cytotoxicity with its effects on the cell membranes: An investigation using langmuir monolayers as membrane models. J. Phys. Chem. B. 118: 10653–10661.

44. Duncan, S.L., and R.G. Larson. 2008. Comparing experimental and simulated pressure-area isotherms for DPPC. Biophys. J. 94: 2965–2986.

45. Jagalski, V., R. Barker, D. Topgaard, T. Günther-Pomorski, B. Hamberger, and M. Cárdenas. 2016. Biophysical study of resin acid effects on phospholipid membrane structure and properties. Biochim. Biophys. Acta - Biomembr. 1858:

2827–2838.

46. Fa, N., L. Lins, P.J. Courtoy, Y. Dufrêne, P. Van Der Smissen, R. Brasseur, D. Tyteca, and M.-P. Mingeot-Leclercq. 2007. Decrease of elastic moduli of DOPC bilayers induced by a macrolide antibiotic, azithromycin. Biochim. Biophys. Acta. 1768: 1830–8.

47. Grancelli, A., A. Morros, M.E. Cabañas, Ò. Domènech, S. Merino, J.L. Vázquez, M.T. Montero, M. Viñas, and J. Hernandez-Borrell. 2002. Interaction of 6-fluoroquinolones with dipalmitoylphosphatidylcholine monolayers and liposomes. Langmuir. 18: 9177–9182.

48. Wüstneck, R., J. Perez-Gil, N. Wüstneck, a Cruz, V.B. Fainerman, and U. Pison. 2005. Interfacial properties of pulmonary surfactant layers. Adv. Colloid Interface Sci. 117: 33–58.

49. Klopfer, K.J.J., and T.K.K. Vanderlick. 1996. Isotherms of Dipalmitoylphosphatidylcholine (DPPC) Monolayers: Features Revealed and Features Obscured. J. Colloid Interface Sci. 182: 220–229.

50. Wieland, D.C.F., P. Degen, T. Zander, S. Gayer, A. Raj, J. An, A. Dėdinaitė, P. Claesson, and R. Willumeit-Römer. 2016. Structure of DPPC–hyaluronan interfacial layers – effects of molecular weight and ion composition. Soft Matter. 12: 729–740.

51. Stefaniu, C., G. Brezesinski, and H. Möhwald. 2012. Polymer-capped magnetite nanoparticles change the 2D structure of DPPC model membranes. Soft Matter. 8: 7952.

52. Soriano, G.B., R. da Silva Oliveira, F.F. Camilo, and L. Caseli. 2017. Interaction of non-aqueous dispersions of silver nanoparticles with cellular membrane models. J. Colloid Interface Sci. 496: 111–117.

53. Goto, T.E., C.C. Lopes, H.B. Nader, A.C.A. Silva, N.O. Dantas, J.R. Siqueira, and L. Caseli. 2016. CdSe magic-sized quantum dots incorporated in biomembrane models at the air-water interface composed of components of tumorigenic and non-tumorigenic cells. Biochim. Biophys. Acta - Biomembr. 1858: 1533–1540.

54. Vaknin, D., K. Kjaer, J. Als-Nielsen, and M. Lösche. 1991. Structural properties

of phosphatidylcholine in a monolayer at the air/water interface: Neutron reflection study and reexamination of x-ray reflection measurements. Biophys. J. 59: 1325–1332.

55. Dietrich, U., P. Krüger, T. Gutberlet, and J.A. Käs. 2009. Interaction of the MARCKS peptide with PIP2in phospholipid monolayers. Biochim. Biophys. Acta - Biomembr. 1788: 1474–1481.

56. Pocivavsek, L., K. Gavrilov, K.D. Cao, E.Y. Chi, D. Li, B. Lin, M. Meron, J. Majewski, and K.Y.C. Lee. 2011. Glycerol-induced membrane stiffening: The role of viscous fluid adlayers. Biophys. J. 101: 118–127.

57. Mohammad-Aghaie, D., E. Macé, C.A. Sennoga, J.M. Seddon, and F. Bresme. 2010. Molecular dynamics simulations of liquid condensed to liquid expanded transitions in DPPC monolayers. J. Phys. Chem. B. 114: 1325–1335.

58. Toimil, P., G. Prieto, J. Miñones, J.M. Trillo, and F. Sarmiento. 2012. Monolayer and Brewster angle microscopy study of human serum albumin-Dipalmitoyl phosphatidyl choline mixtures at the air-water interface. Colloids Surfaces B Biointerfaces. 92: 64–73.

59. Brezesinski, G., A. Dietrich, B. Struth, C. Böhm, W.G. Bouwman, K. Kjaer, and H. Möhwald. 1995. Influence of ether linkages on the structure of double-chain phospholipid monolayers. Chem. Phys. Lipids. 76: 145–157.

60. Gericke, A., C.R. Flach, and R. Mendelsohn. 1997. Structure and orientation of lung surfactant SP-C and L-alpha-dipalmitoylphosphatidylcholine in aqueous monolayers. Biophys. J. 73: 492–499.

61. Takeshita, N., M. Okuno, and T. Ishibashi. 2017. Molecular conformation of DPPC phospholipid Langmuir and Langmuir–Blodgett monolayers studied by heterodyne-detected vibrational sum frequency generation spectroscopy. Phys. Chem. Chem. Phys. 19: 2060–2066.

62. Estrela-Lopis, I., G. Brezesinski, and H. Möhwald. 2004. Miscibility of DPPC and DPPA in monolayers at the air/water interface. Chem. Phys. Lipids. 131: 71–80.

63. Iskander, S. 2011. Axisymmetric Drop Shape Analysis (Adsa) and Lung Surfactant. .

64. Kosol, S., E. Schrank, M.B. Krajačić, G.E. Wagner, N.H. Meyer, C. Göbl, G.N. Rechberger, K. Zangger, and P. Novak. 2012. Probing the interactions of macrolide antibiotics with membrane-mimetics by NMR spectroscopy. J. Med. Chem. 55: 5632–5636.

65. Goldman, R.C., S.W. Fesik, C.C. Doran, A. Laboratories, and A. Park. 1990. Role of Protonated and Neutral Forms of Macrolides in Binding to Ribosomes from Gram-Positive and Gram-Negative Bacteria. Antimicrob. Agents Chemother. 34: 426–431.

66. Schlunzen, F., R. Zarivach, J. Harms, A. Bashan, A. Tocilj, R. Albrecht, A. Yonath, and F. Franceschi. 2001. Structural basis for the interaction of antibiotics with the peptidl transferase centre in eubacteria. Nature. 413: 814–821.

67. C. Peetla, A. Stine, V.L. 2009. Biophysical interactions with model lipid membranes: applications in drug discovery and drug delivery. Mol Pharm. 6: 1264–1276.

68. Bensikaddour, H., K. Snoussi, L. Lins, F. Van Bambeke, P.M. Tulkens, R. Brasseur, E. Goormaghtigh, and M.-P.P. Mingeot-Leclercq. 2008. Interactions of ciprofloxacin with DPPC and DPPG: fluorescence anisotropy, ATR-FTIR and 31P NMR spectroscopies and conformational analysis. Biochim. Biophys. Acta. 1778: 2535–43.

69. Mitscher, L.A. 2005. Bacterial topoisomerase inhibitors: Quinolone and pyridone antibacterial agents. Chem. Rev. 105: 559–592.

70. Lambert, A., J.B. Regnouf-de-Vains, and M.F. Ruiz-López. 2007. Structure of levofloxacin in hydrophilic and hydrophobic media: Relationship to its antibacterial properties. Chem. Phys. Lett. 442: 281–284.

71. Hirano, T., S. Yasuda, Y. Osaka, M. Kobayashi, S. Itagaki, and K. Iseki. 2006. Mechanism of the inhibitory effect of zwitterionic drugs (levofloxacin and grepafloxacin) on carnitine transporter (OCTN2) in Caco-2 cells. Biochim. Biophys. Acta - Biomembr. 1758: 1743–1750.

72. Montero, M.T., S. Merino-montero, and T. Vinuesa. 2006. Interfacial Membrane Effects of Fluoroquinolones as Revealed by a Combination of Fluorescence Binding Experiments and Atomic Force Microscopy Observations. Langmuir.

22: 7574–7578.

73. Fresta, M., S. Guccione, A.R. Beccari, P.M. Furneri, and G. Puglisi. 2002. Combining molecular modeling with experimental methodologies: Mechanism of membrane permeation and accumulation of ofloxacin. Bioorganic Med. Chem. 10: 3871–3889.

74. Marsh, D. 1996. Lateral pressure in membranes. Biochim. Biophys. Acta - Rev. Biomembr. 1286: 183–223.

Figure Captions

Figure 1. Molecular structures of the antibiotics used in this study.

Figure 2. (A) Surface pressure-area (π-A) isotherms of pure (black) and mixed DPPC/Clarithromycin monolayers at 10 % w/w (blue); 1 % (green) and 0.1 % (red). (B) surface compressional modulus at the air-water interface calculated from the isotherms in (A). (C) Surface pressure-area (π-A) isotherms of pure DPPC (black) and mixed DPPC/Levofloxacin at 10 % w/w (blue); 1 % (green) and 0.1 % (red). (D) surface compressional modulus at the air-water interface from the isotherms in (B).

Figure 3. Brewster angle microscopy images of pure DPPC (1 $g.L^{-1}$) (A) 0 mNm^{-1} and (B) 30 mNm^{-1}. Mixed DPPC/Clarithromycin at 0 mNm^{-1} (C 0.1% w/w; D 1%; E 10%) and 30 mNm^{-1} (F 0.1% w/w; G 1%; H 10%). Mixed DPPC/Levofloxacin at 0 mNm^{-1} (I 0.1% w/w; J 1%; K 10%) and 30 mNm^{-1} (L 0.1% w/w; M 1%; N 10%). All BAM images have a 25 μm scale bar at the left hand corner.

Figure 4. Experimental PM-IRRAS spectra of Langmuir films of pure DPPC (black solid line), DPPC/Levofloxacin 0.1% w/w (green dot-dashed line), DPPC/levofloxacin 10% w/w (brown double-dashed-dot line), DPPC/ Clarithromycin 0.1% w/w (red dashed line) and DPPC/ Clarithromycin 10% w/w (blue dot line) at the head groups region (1450–1800 cm^{-1}) and a surface pressure of 30 mNm^{-1}.

Figure 5. Neutron Reflectometry data and the best two-layer fittings from simultaneous fitted d-DPPC on ACMW (green) and h-DPPC on D_2O (blue) monolayers at the air-water interface and a surface pressure of 30 mNm^{-1}. Upper figure: Reflectivity vs Q ($Å^{-1}$), Lower figure: The scattering length density plot of all contrasts vs the distance from the interface.

Figure 6. Neutron Reflectometry data and the best two-layer fittings obtained from simultaneous fitted h-DPPC/Clarithromycin on D_2O (orange); d-DPPC/Clarithromycin on D_2O (blue) and d-DPPC/Clarithromycin on ACMW (green) 10% w/w monolayers at the air-water interface and surface pressure of 30 mNm^{-1}. Upper Figure: Reflectivity vs Q ($Å^{-1}$). Lower Figure: The scattering length density plot of all contrasts vs the distance from the interface.

Figure 7. Neutron Reflectometry data and the best two-layer fittings from simultaneous fitted h-DPPC/Levofloxacin on D_2O (orange); d-DPPC/Levofloxacin on D_2O (blue) and d-DPPC/Levofloxacin on ACMW (green) 10% w/w monolayers at the air-water interface

and a surface pressure of 30 mNm^{-1}. Upper Figure: Reflectivity vs Q ($Å^{-1}$), Lower Figure: The scattering length density plot of all contrasts vs the distance from the interface.

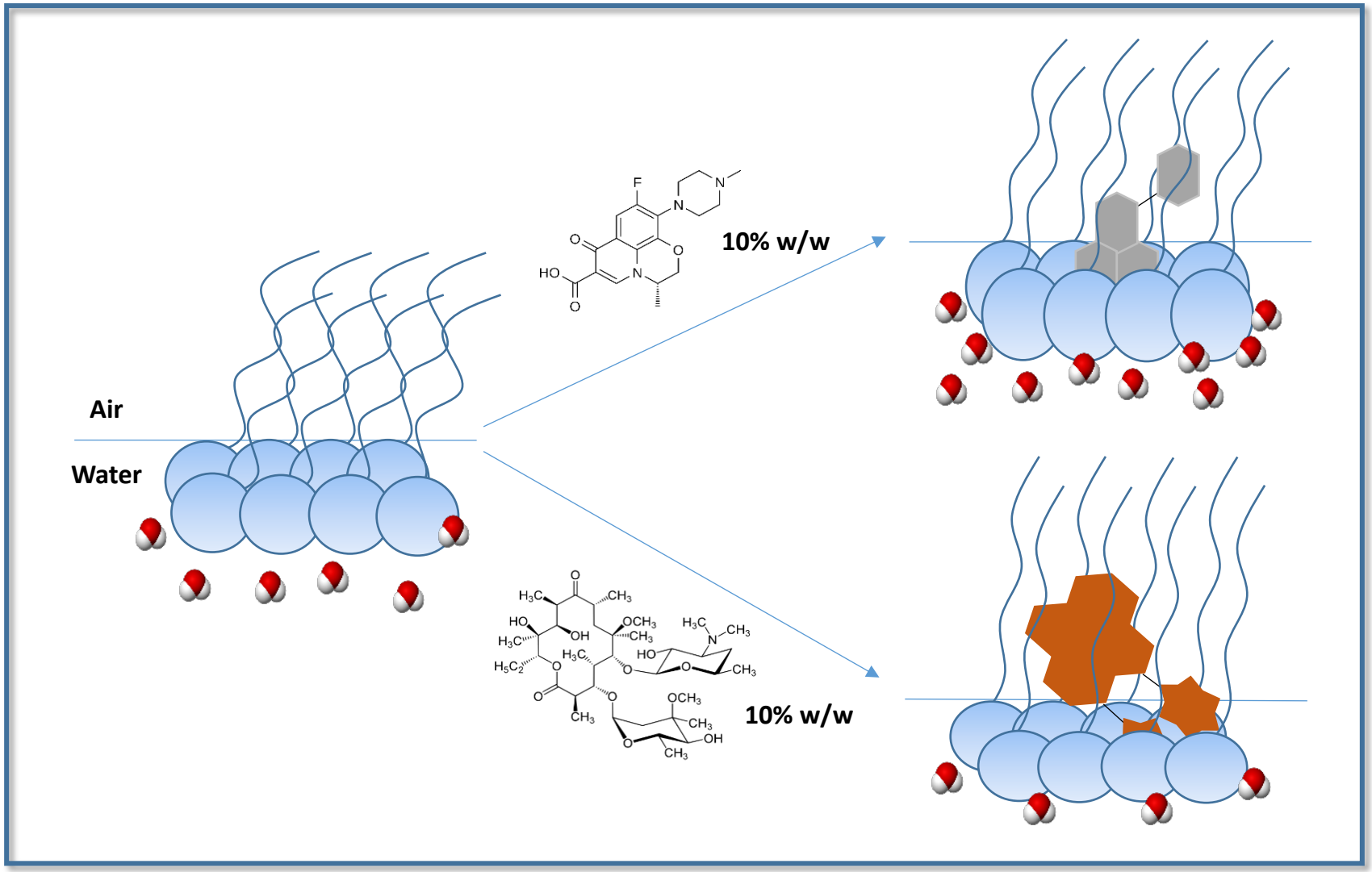

Table of Contents Graphic